Electronic Supplementary Information (ESI) for Chem. Comm.

PVP-assisted Transformation of Metal–Organic Framework into Co-Embedded N-Enriched Meso/Microporous Carbon Materials as Bifunctional Electrocatalysts

Zuozhong Liang,[a] Chaochao Zhang,[a] Haitao Yuan,[a] Wei Zhang,[a] Haoquan Zheng,*[a] and Rui Cao*[ab]

[a]School of Chemistry and Chemical Engineering, Shaanxi Normal University, Xi'an, 710119, China.
[b]Department of Chemistry, Renmin University of China, Beijing, 100872, China.

Correspondence Email: zhenghaoquan@snnu.edu.cn; ruicao@ruc.edu.cn

1. Experimental section

1.1 Materials

All chemicals were used as received without any further purification. $Co(NO_3)_2 \cdot 6H_2O$ (99.99%) and 2-methylimidazole (%) were purchased from the Energy Chemical. Methanol (AR, 99.5%) was purchased from the Tianjin Fuyu Fine Chemical Co., Ltd. KOH (98%) was purchased from Sinopharm Group Chemical Reagent Co., Ltd.

1.2 Preparation of porous Co-NC Materials

First, 1 mmol $Co(NO_3)_2 \cdot 6H_2O$ (0.291 g) and 4 mmol 2-methylimidazole (0.238 g) was separately dissolved in 25 mL methanol and sonicated for 5 mins. Then, 2 mmol PVP k30 (160 mg) were added into the prepared Co solution and stirring for 5 mins. The as-prepared 2-methylimidazole solution was slowly dropped into the above solution under the stirring. The resulting slurry was aging for 24 h. The obtained product was denoted as P-ZIF-67-2. In contrast, the product without adding the PVP, namely ZIF-67, and with adding 4, 6, 8 mmol PVP, namely P-ZIF-67-4, P-ZIF-67-6, and P-ZIF-67-8, were synthesized and calcinated with the same method. Then the as-prepared particles were heated to 800 °C at a rate of 5 °C min^{-1} in a tube furnace under N_2 atmosphere for 2 h. The final products were defined as Co-NC, P-Co-NC-2, P-Co-NC-4, P-Co-NC-6, and P-Co-NC-8, respectively.

1.3 Characterization

Powder X-ray diffraction (PXRD) patterns of as-prepared materials were measured with a X-ray diffractometer (Bruker, D8 Advance, Cu Kα, λ = 1.5406 Å, 40 kV/40mA). The morphology of the as-prepared material was observed with scanning electron microscopy (SEM, Hitachi, SU8020) and transmission electron microscopy (TEM, JEOL, JEM-2100). The Brunauer-Emmett-Teller (BET) specific surface area was measured in Micromeritics ASAP 2020. The X-ray photoelectron spectroscopy (XPS) analysis of the prepared materials was performed with a Kratos AXIS ULTRA XPS. Thermogravimetric analysis (TGA) was applied by heating the as-prepared sample at a rate of 10 °C min^{-1} with N_2 and air from 20 °C to 1000 °C in a TA Instruments SDT Q600. Elemental analyzer (Vario EL III, Elementar Analysensysteme GmbH) was applied to measure the content of C, H, and N. The Raman spectra were measured with a Raman Spectrometer (inVia Reflex, Renishaw).

1.4 Electrochemical measurement

All the electrochemical measurements of ORR performance were performed at ~ 25 °C with a CHI 760E Electrochemical Analyzer (CH Instruments) and a Pine Modulated

Speed Rotator (Pine Research Instrumentation, Inc.). In particular, we selected the rotating ring-disk electrode (RRDE) as the working electrode, Pt wire as the auxiliary electrode, and saturated Ag/AgCl as the reference electrode. In a typical procedure, 5 mg of catalysts and 10 μL of Nafion solution (5 wt%, DuPont) were added into 1 mL of isopropanol/deionized water (DIW) solution ($V_{isopropanol}$: V_{DIW} = 450 : 40) and then ultrasonicated for ~ 1 h to prepare a homogeneous slurry. Finally, 20 μL of the catalysts was coated onto the RDE electrode using pipette (catalyst loading: ~ 0.4 mg cm^{-2}) and dried naturally to form a homogeneous membrane. For the ORR, the cyclic voltammetry (CV) measurements were carried out in O_2/N_2-saturated 0.1 M KOH solution at ~ 25 °C with a scan rate of 5 mV s^{-1}. The linear sweep voltammetry (LSV) measurements were performed in O_2-saturated 0.1 M KOH solution at different rotating rate from 400 to 1600 rpm.

The kinetic properties of the ORR were carried out with the rotating ring-disk electrode (RRDE) in O_2-saturated 0.1 M KOH solution at ~ 25 °C with a scan rate of 5 mV s^{-1} and the ring-electron potential was held at 1.5 V vs RHE. The diameter of the disk is 5.61 mm (0.247 cm^2) and the area of the ring is 0.186 cm^2. The transfer electron number (n) was calculated with the following equation:

$$n = 4\frac{i_d}{i_d + i_r/N}$$

where i_d is the disk current, i_r is the ring current, and N is the ring current collection efficiency, which was deterimined to be ~ 0.39 with the LSV measurement in $K_3Fe[CN]_6$ solution. The peroxide percentage (%H_2O_2) can be calculated with the following equation:

$$\%H_2O_2 = 200\frac{i_r/N}{i_d + i_r/N}$$

.

For the OER testing, the activities of the as-prepared materials were evaluated with a CHI 660E Electrochemical Analyzer (CH Instruments). Cyclic voltammetry (CV) curves of the as-prepared catalysts were measured in 1.0 M KOH solution with a three-electrode system. We selected the glassy carbon (GC) electrode with a diameter of 3 mm (0.07 cm^2) as the working electrode, Pt wire as the auxiliary electrode, and saturated Ag/AgCl as the reference electrode. In a typical procedure, 4 mg of catalysts and ~ 30 μL of Nafion solution (5 wt%, DuPont) were added into 1 mL of DIW/ethanol solution (V_{DIW} : $V_{ethanol}$ = 2 : 1) and then ultrasonicated for ~ 1 h to prepare a

homogeneous slurry. Finally, 5 μL of the as-prepared catalysts was coated onto the GC electrode using pipette. The overpotential (η) was calculated based on the following equation:

$$\eta = E_{Ag/AgCl} + (0.197 + 0.059 \times pH) - 1.23.$$

Table S1. The electron transfer number (*n*) for the commercial Pt/C and as-prepared catalysts Co-NC, P-Co-NC-4, and P-Co-NC-8 measured in O_2-saturated 0.1 M KOH solution at a rotation rate of 1600 rpm.

Catalysts	0.2 V	0.3 V	0.4 V	0.5 V	0.6 V	0.7 V	0.8 V
Pt/C	3.95	3.97	3.97	3.97	3.98	3.98	4.00
Co-NC	3.55	3.60	3.64	3.68	3.75	3.84	3.82
P-Co-NC-4	3.49	3.55	3.60	3.67	3.77	3.88	3.89
P-Co-NC-8	3.41	3.44	3.48	3.49	3.57	3.68	3.82

Table S2. Electrochemical activities of bifunctional oxygen catalysts in this work and other reported works.

Electrocatalysts	*E* (OER) at 10 mA cm^{-2}		$E_{1/2}$ (ORR) in 0.1 M KOH	Reference
	1.0 M KOH	0.1 M KOH		
P-Co-NC-4	**315 mV**	**360 mV**	**850 mV**	**This work**
Co_3O_4@C-MWCNTs	320 mV	–	810 mV	*J. Mater. Chem. A, 2015, 3, 17392–17402*
Fe_3C@NCNT/NPC	340 mV	–	900 mV	*Catal. Sci. Technol., 2016, 6, 6365–6371*
Co-MOF@CNTs	340 mV	–	820 mV	*J. Power Sources 326 (2016) 50-59*
ZnCoNC-0.1	–	520 mV	840 mV	*Nano Res. 2018, 11(1): 163–173*
Co/NC	–	460 mV	830 mV	*Angew. Chem. Int. Ed. 2016, 55, 4087–4091*
Co@Co_3O_4/NC-2	–	435 mV	810 mV	*Appl. Surf. Sci. 427 (2018) 319–327*
Co@N-C	–	350 mV	817 mV	*Adv. Mater. 2018, 1705431*
Co@Co_3O_4/NC	–	420 mV	800 mV	*Angew. Chem. Int. Ed. 2016, 55, 4087–4091*
Co_3O_4@Co/NCNT	–	380 mV	860 mV	*Chem. Eur. J. 2017, 23, 18049–18056*
$Ni_xCo_yO_4$/Co–NG	–	399 mV	804 mV	*J. Mater. Chem. A, 2017, 5, 5594–5600*

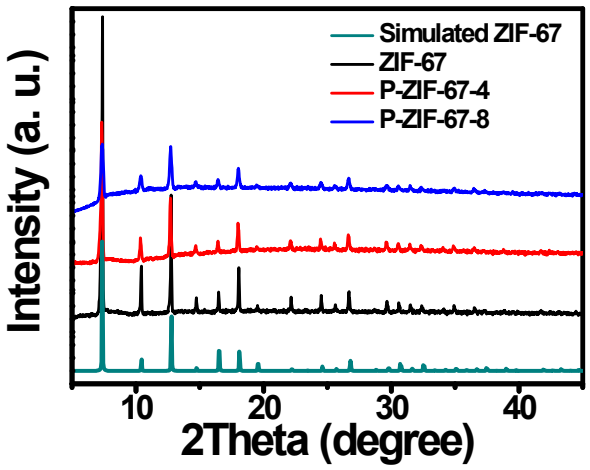

Fig. S1. XRD patterns of simulated ZIF-67, ZIF-67, P-ZIF-67-4, and P-ZIF-67-8.

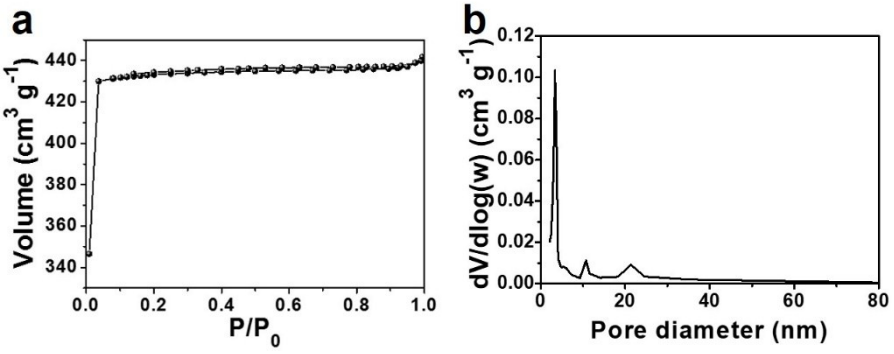

Fig. S2. N_2 adsorption-desorption isotherms (a) and pore size distribution (b) for the as-prepared P-ZIF-67-8.

The BET surface area of the as-prepared P-ZIF-67-8 is 1351.49 m²/g.

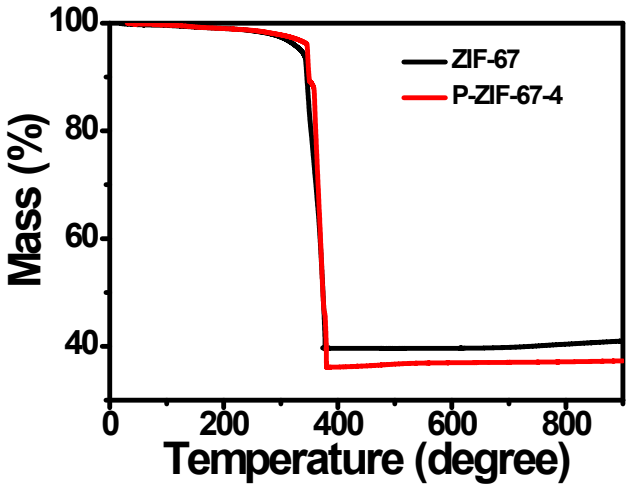

Fig. S3. Thermogravimetric analysis (TGA) curves of ZIF-67 (black) and P-ZIF-67-4 (red) measured in air.

The encapsulation of PVP in the P-ZIF-67-4 leads to the lower mass after pyrolysis in air. This is because PVP decomposes with a low carbonization yield of 4% during pyrolysis.

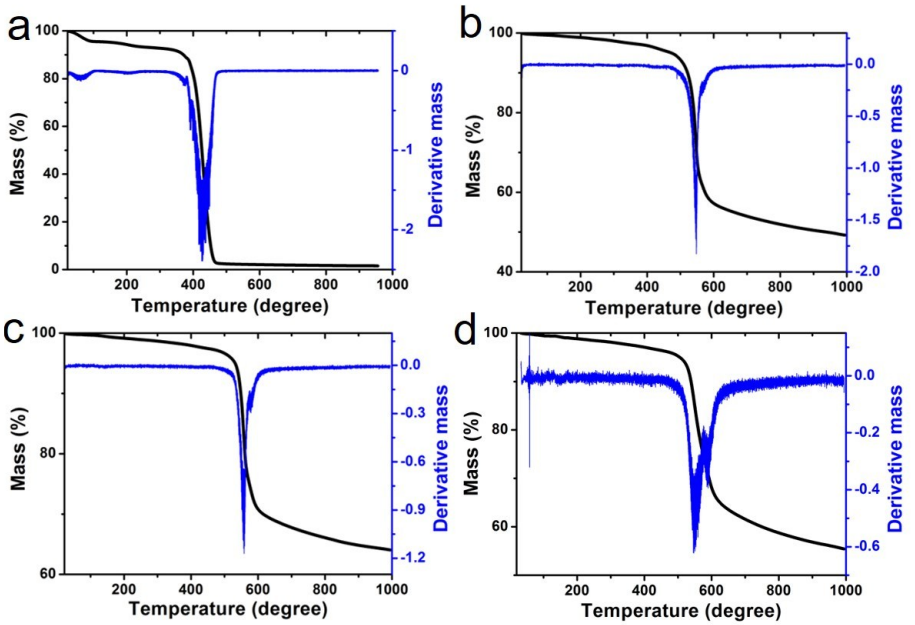

Fig. S4. TGA and the corresponding derivative TG curves of PVP (a), ZIF-67 (b), P-ZIF-67-4 (c), and P-ZIF-67-8 (d) measured in N_2.

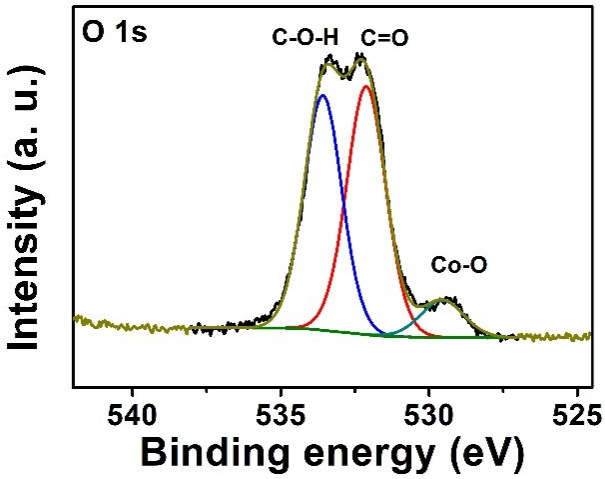

Fig. S5. High-resolution XPS spectrum of O 1s for the P-Co-NC-4.

The O1s XPS spectrum of the P-Co-NC-4 can be deconvoluted into the peaks for Co-O (529.6 eV), C=O bonds (532.1 eV) and C-O-H group (533.6 eV).

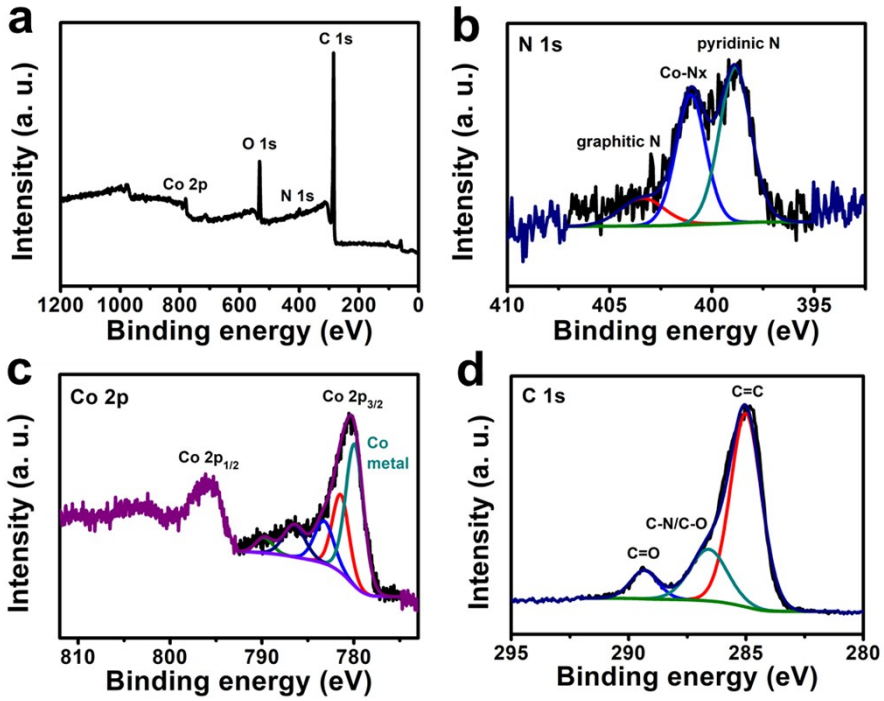

Fig. S6 XPS survey (a) and high-resolution spectra of N 1s (b), Co 2p (c), and C 1s (d) for the Co-NC.

The XPS spectra of Co-NC prepared without PVP were measured and the results are shown in Fig. S6. It is found that the graphitic N content of high resolution XPS spectrum of N 1s for P-Co-NC-4 (24%) is higher than that in Co-NC (14%), which is consistent with the increased N content of P-Co-NC-4 and the formation of interfacial structure induced by PVP.

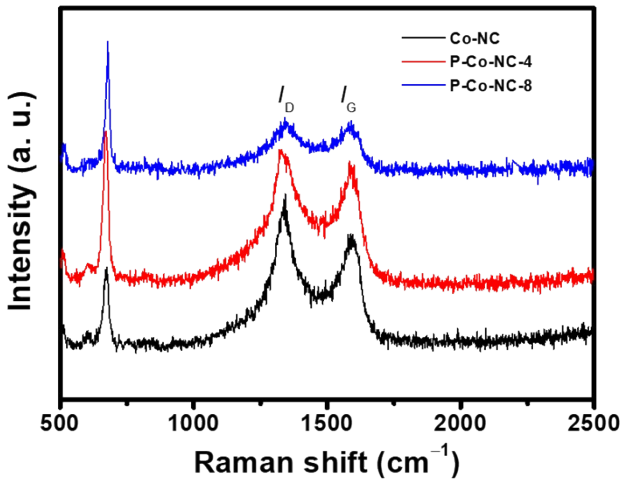

Fig. S7 Raman spectra of as-prepared Co-NC, P-Co-NC-4, and P-Co-NC-8.

The I_D/I_G is 1.29, 1.08 and 1.04 for the Co-NC, P-Co-NC-4, and P-Co-NC-8, respectively. There are less C defects in materials with the increasing of PVP, which can be attributed to the formation of the defect-less stable PVP derived carbon//ZIF-67 interfacial structure in P-Co-NC-4 and P-Co-NC-8.

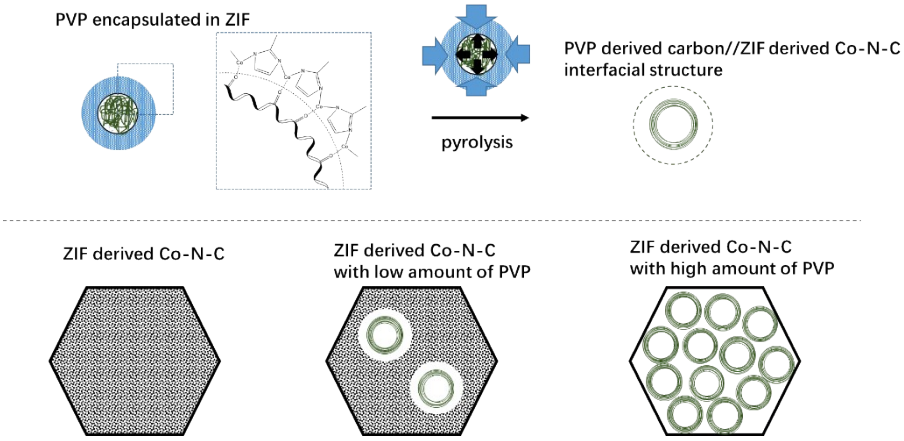

Fig. S8. Scheme illustration of the formation process of a PVP derived carbon//ZIF-67 derived carbon interfacial structure.

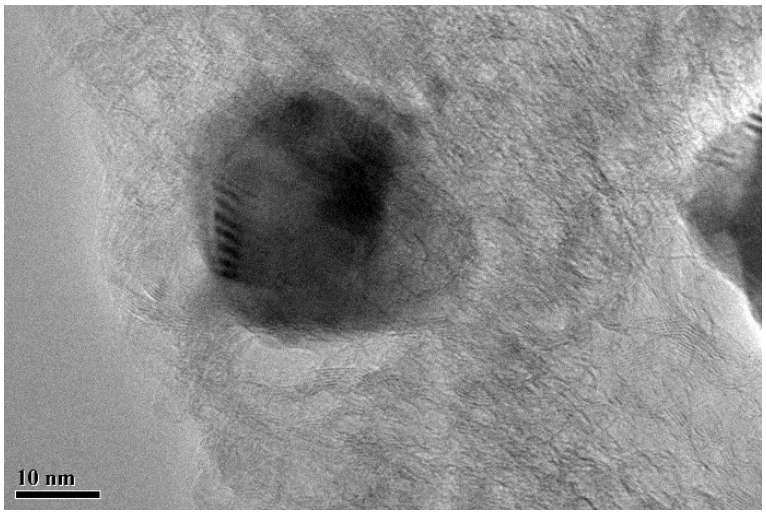

Fig. S9. HRTEM image of the as-prepared P-Co-NC-8.

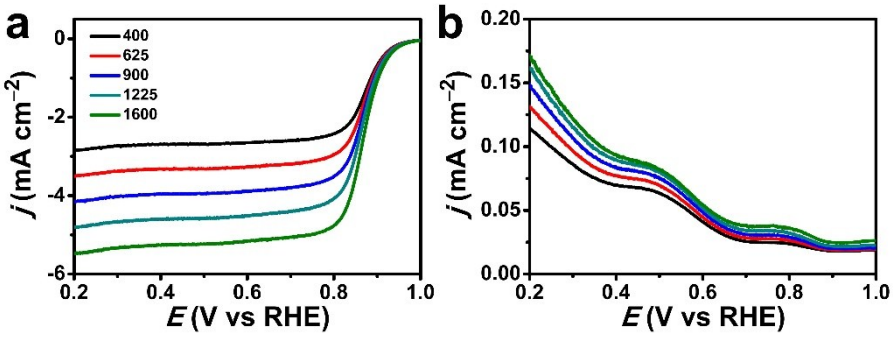

Fig. S10. RRDE measurements of LSV curves for the Pt/C after pyrolysis with different rotation rates in O_2-saturated 0.1 M KOH solution at a scan rate of 10 mV s^{-1} (a: the current density for the disk; b: the current density for the ring).

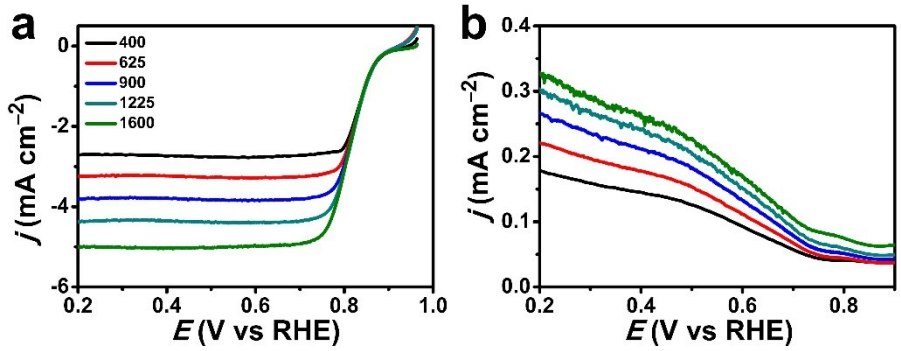

Fig. S11. RRDE measurements of LSV curves for the Co-NC with different rotation rates in O_2-saturated 0.1 M KOH solution at a scan rate of 10 mV s^{-1} (a: the current density for the disk; b: the current density for the ring).

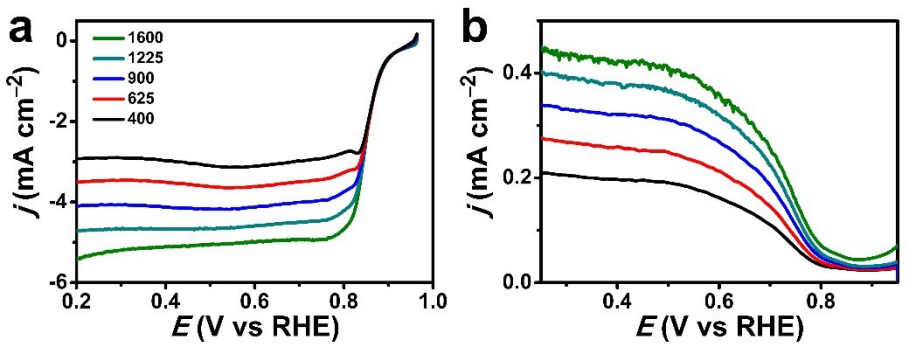

Fig. S12. RRDE measurements of LSV curves for the P-Co-NC-4 with different rotation rates in O_2-saturated 0.1 M KOH solution at a scan rate of 10 mV s^{-1} (a: the current density for the disk; b: the current density for the ring).

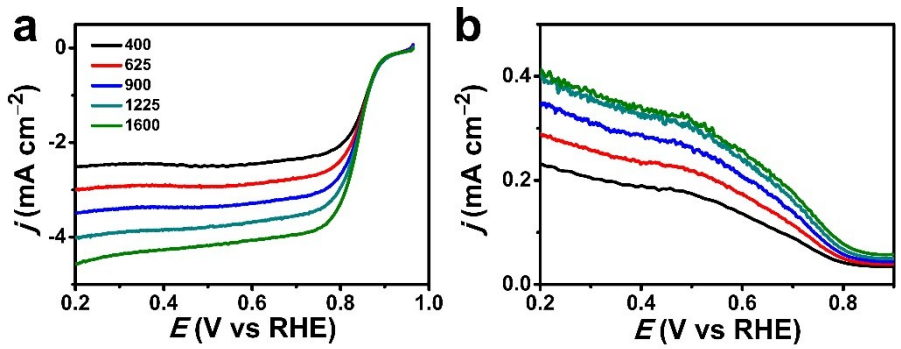

Fig. S13. RRDE measurements of LSV curves for the P-Co-NC-8 with different rotation rates in O_2-saturated 0.1 M KOH solution at a scan rate of 10 mV s^{-1} (a: the current density for the disk; b: the current density for the ring).

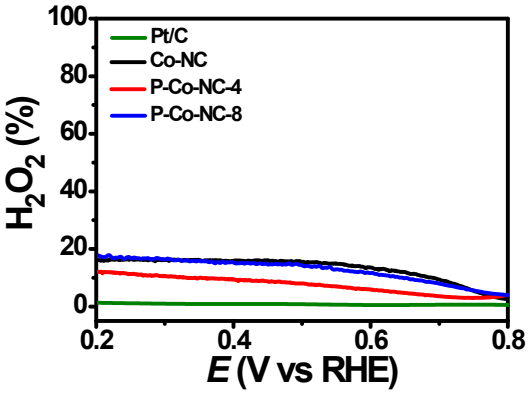

Fig. S14. H_2O_2 yield of Pt/C, Co-NC, P-Co-NC-4, and P-Co-NC-8 at various potentials based on RRDE data.

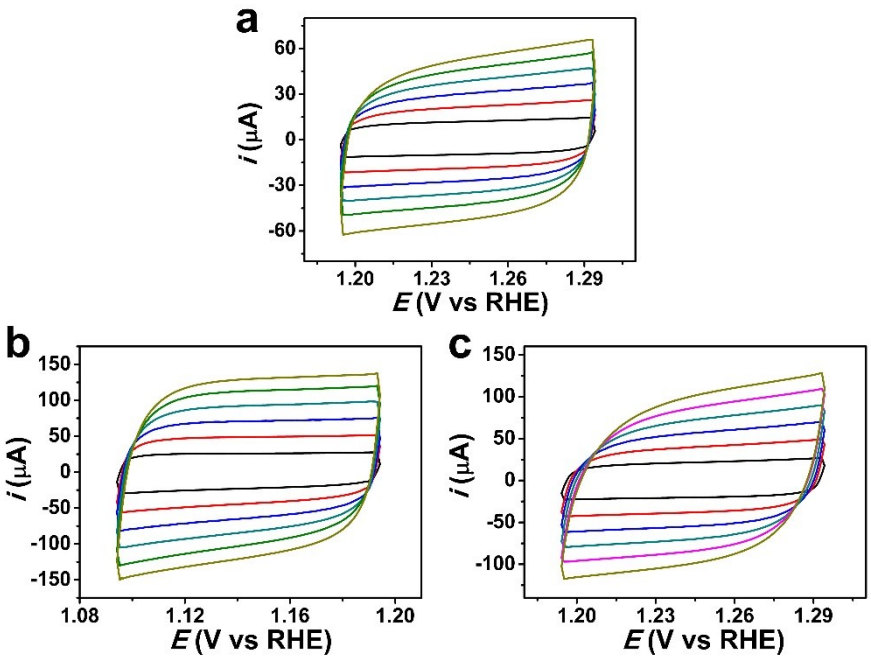

Fig. S15. CVs of Co-NC (a), P-Co-NC-4 (b) and P-Co-NC-8 (c) at scan rates of 20, 40, 60, 80, 100, and 120 mV s^{-1}.